9.8 LOW-LEVEL CLOUD VARIABILITY OVER THE EQUATORIAL COLD TONGUE

David K. Mansbach* and Joel R. Norris

Scripps Institution of Oceanography, University of California, San Diego

1. INTRODUCTION

Low clouds combine a small greenhouse effect with a generally high albedo and contribute significantly to the overall net cooling role of clouds in Earth's climate (Ramanathan et al. 1989). By examining the interannual variability of low clouds in the eastern equatorial Pacific, an area of high atmospheric and oceanic variability located on the edge of a persistent stratiform deck, we aim to uncover sometimes-subtle details of low marine cloud processes and ocean-air feedbacks.

Climatologically, low stratiform clouds are found in subtropical subsidence regions over the relatively cool east side of oceans, and they are most prevalent in seasons of low sea surface temperature (SST) and high lower-tropospheric stability (LTS) (Klein and Hartmann 1993).

Since cold air advection by trade winds predominates in the marine subtropics, cold advection has been more common in observational analysis, theory, and models. A dramatic example of cold air advection is the sudden transition found in the eastern Pacific from cool, upwelled waters to warmer ones north of the equatorial SST as in Deser et al. (1993). The strong climatological cold advection in this area leads to rapid increases in sea-air latent and sensible heat fluxes and results in meridional shifts in cloud type and sea-air temperature difference, as well as cloudiness patterns that track with the location of the sharp SST gradient (Deser et al. 1993; Norris 1998b).

Although warm air advection is less common in the subtropics, the cases where it occurs can shed light on boundary-layer atmospheric physics and the nature of air-sea coupling. In this study we examine cloudiness over the southeastern tropical Pacific, where there is climatological warm-air advection as southeasterly trade winds approach the equatorial cold tongue. The area encompasses the northern edge of the extensive southeastern Pacific stratiform cloud region, and we focus on the cloud response to interannual oceanic and atmospheric fluctuations. By examining the case of warm-air advection, we gain insight into factors important to low cloud amount other than SST and LTS.

2. DATA

We draw on monthly-mean cloud data averaged over all available daytime retrievals from the International Satellite Cloud Climatology Project (ISCCP) D2 dataset, on a 2.5° grid from July 1983-September 2001 (Rossow and Schiffer 1999). For meteorological and SST data we use the National Centers for Environmental Prediction-National Center for Atmospheric Research (NCEP-NCAR) reanalysis data (Kalnay et al. 1996) monthly-mean fields.

We also examine data from ship-based surface observers collected in the Extended Edited Cloud Report Archive (EECRA) (Hahn and Warren 1999) from 1952-1997. Observations in the EECRA include sky coverage or clear sky at different heights, cloud type, SST, and air temperature.

Two sets of soundings come from cruises affiliated with the Eastern Pacific Investigation of Climate Processes in the Coupled Ocean-Atmosphere System (EPIC) program. We present composite soundings from transects in October of 1999 and 2001 along both 95 and 110°W [described in Pyatt et al. (2005)].

We also examine whether modern global coupled climate models (GCCM) show cloud behavior similar to that in observations. The Geophysical Fluid Dynamics Laboratory of the National Oceanic and Atmospheric Administration recently released data from runs of its coupled model versions 2.0 and 2.1 (denoted GFDL 2.0 and GFDL 2.1, respectively). The two model versions are similar, differing mainly in their atmospheric dynamical core (with GFDL 2.1 employing a finite volume core) as well as cloud tuning and details in the land and ocean models as described in Delworth et al. (2005). Since both versions have certain advantages and represent latest-generation coupled climate models, we evaluate data from both. We also evaluate another, separately developed GCCM, the Community Climate System Model 3.0 (CCSM 3.0) (Collins et al. 2005).

3. PROCESSING TECHNIQUES

For all data, we restrict our analysis to the months June-November, when southeast Pacific low clouds are considerably more abundant. In the ISCCP data, “low" refers to clouds whose tops are at a pressure greater than 680 hPa, and we look at low cloud coverage of all optical thicknesses. Since a satellite cannot see low-level clouds when upper-level clouds are obscuring its view, we correct ISCCP data by assuming that low-level clouds are randomly overlapped with upper-level (middle plus high) clouds. Taking observed upper-level cloud cover, U, and observed low-cloud cover, L, into account, we compute L', the corrected low cloud amount, from $L'=L\,(1-U)^{-1}$.

* Corresponding author address: David K. Mansbach, Scripps Institution of Oceanography, La Jolla, CA 92093-0224; e-mail: dmansbach@ucsd.edu

We subtract climatological monthly data and examine interannual anomalies of the cloud and meteorological data. Local correlation between low cloud amount and several meteorological fields are examined. Following Klein and Hartmann (1993), we define lower-tropospheric stability (LTS) as the difference in potential temperature at 700hPa and the surface, $\theta_{700} - \theta_{sfc}$.

Since low cloud amount is related to more than just one atmospheric quantity, we also use multilinear regression to see how much additional low cloud amount variability a second atmospheric variable can explain. For instance, at each grid box we run a linear model to see how much low cloud variance is explained (i.e., the value of the R^2 statistic) by LTS. We then use surface-layer-temperature advection, calculated using reanalysis surface-layer winds and SST, as a second regressor, and see how much more variance is explained. The results indicate total variance explained by linear methods as well as showing how independent the two regressors are.

As shown below, our analysis indicates the importance of atmospheric temperature advection within a specific area over the cold tongue. Rather than rely on linear analysis, since we want also resolve the variables that do not vary linearly with temperature advection, we instead use compositing analysis to examine the changes in cloud, ocean, and atmospheric variables corresponding to temperature advection anomalies. After defining a cold tongue box over which temperature advection seems particularly important, we group the temperature advection anomaly values into quintiles and examine the corresponding mean values of other

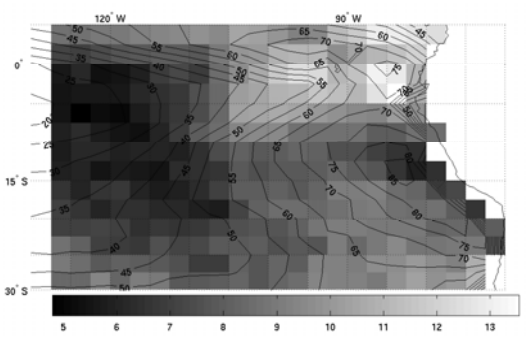

Fig. 1. June-November mean low cloud amount (contours) and standard deviation of interannual anomalies (shading) from ISCCP data.

variables for high and low quintiles, both on a grid-box-by-grid-box basis and as a zonal average over the region from 105°-95°W.

The confidence levels presented for all zonal averages are computed using bootstrap resampling methods. For 10000 realizations we construct physically feasible subsets of data taken from the complete data sets, and determine the 95% confidence levels as the values surrounding the central 9500 subset means. For the EECRA data, half of the observations were taken to be independent, while for zonally averaged ISCCP data another method was used. We calculate $N_{eff} = -N(2\ln(\rho))^{-1}$, where N is the number of monthly observations and ρ is the one-month autocorrelation. We then round off the

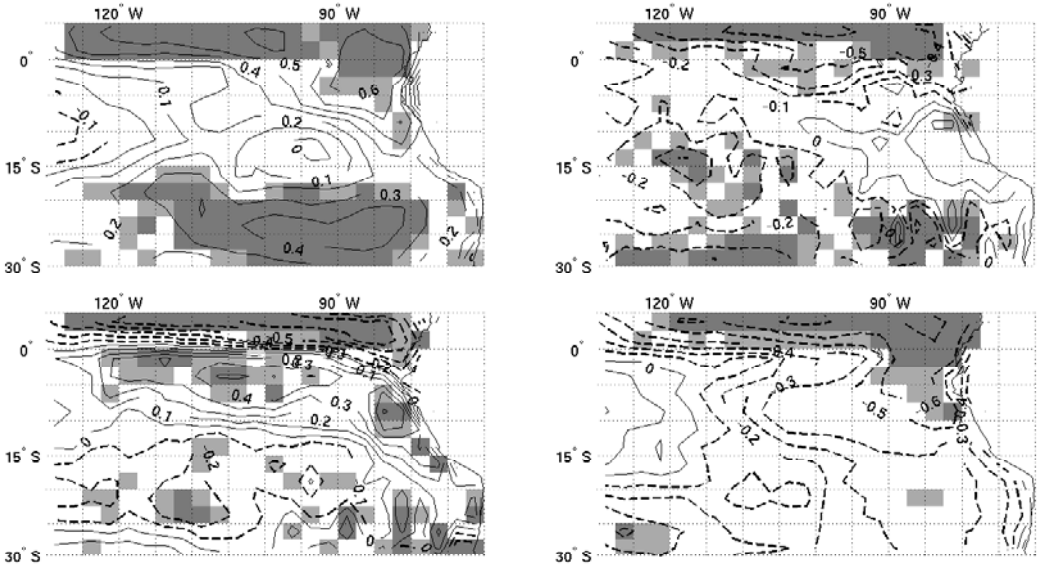

Fig.2. Correlation (contoured) between (upper-left) ISCCP low clouds and lower tropospheric stability anomalies; (upper-right) low clouds and atmospheric temperature advection anomalies; (lower-left) lower tropospheric stability and temperature advection; and (lower-right) SST and low cloud anomalies. Shading indicates significance at the 95% (light shading) and 99% (dark shading) confidence levels.

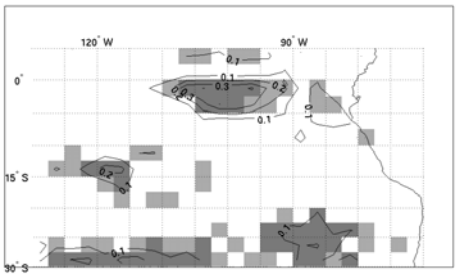

Fig. 3. Increase in variance explained(R^2) by regressing with anomalous surface-layer atmospheric temperature advection as well as anomalous lower tropospheric stability. Shading indicates significance at the 95% (light shading) and 99% (dark shading) confidence levels.

quantity N/N_{eff} and adjudge months in each quintile that are within this many months of each other to be dependent. Months from different years are always considered independent with this method.

With the EPIC data, for each sounding we compute equivalent and virtual potential temperatures as well as water vapor mixing ratio using the methods of Bolton (1980), then average all soundings within the equatorial Pacific domain of interest. Since taking a simple mean tends to smooth out the trade inversion, we use a different approach. First, we limit the analysis to those soundings with an inversion, although this requires discarding few of the soundings. In order to average, we scale the height coordinate by the altitude of the trade inversion base, which we define objectively as the lowest height where the subsequent 10 data readings (usually about 200 vertical meters) are greater in temperature and the temperature rises to at least 1.5K greater than at the inversion base. We then take the mean values of the scaled sounding data, and present the mean corresponding heights in our plots.

Our comparison with model data as well is based on local correlation analysis and compositing analysis. Just as with the observations, with the model output we calculate surface-layer atmospheric temperature advection and examine conditions occurring during warmest and coldest quintile months in the area where the model demonstrates advection and low cloud variability conditions most similar to those in the area of interest in the observations.

From observational and model data, we present zonally averaged values reflecting mean cloud amounts in warm and cool temperature advection anomaly regimes. This provides a compact representation of the observed phenomena and straightforward way of determining whether these phenomena are simulated properly. Many of the calculations made with the observations, particularly the reanalysis and ISCCP, were also repeated with the model data, although in the interest of compactness many results are not shown.

4. ISCCP RESULTS

Fig. 1 gives the mean low cloud distribution and standard deviation of interannual anomalies from ISCCP data. The heart of the dense low cloud region aligns with areas of cooler waters off the South American coast, with a secondary pronounced area of low cloud north of the SST front. This area north of the Equator is also an area of high interannual variability, which is consistent with low cloudiness developing with climatological cold advection and varying with the strength of the equatorial front, El Niño-Southern Oscillation (ENSO) events, and tropical instability waves (Deser et al. 1993).

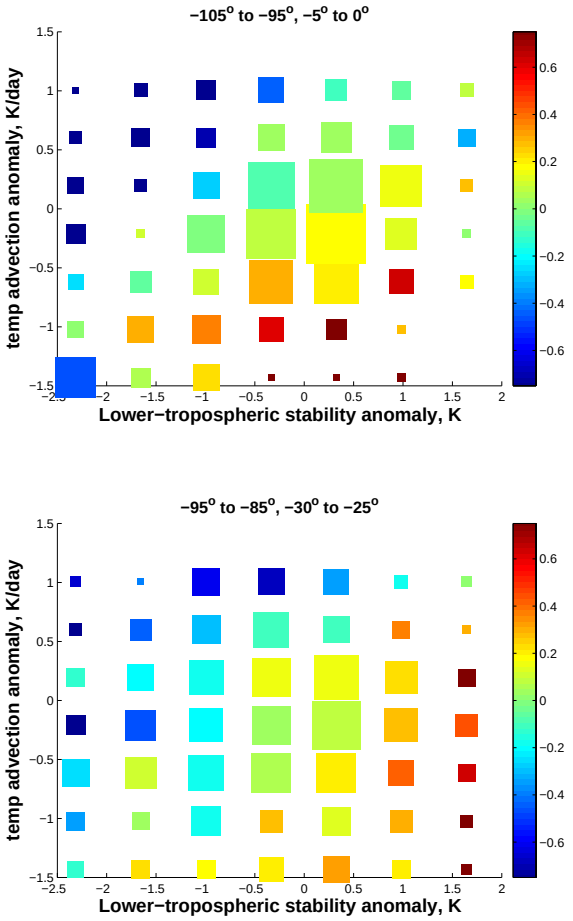

Fig. 4 Colors indicate mean normalized ISCCP low cloud anomaly as a function of lower-tropospheric stability and surface layer temperature advection anomalies. Area of each square indicates the number of grid box-months that were used to make the mean values. Top: 105°-95°W, 5°S - 0° bottom: 95°-85° W, 30°-25°S.

Another area of elevated standard deviation around 25°S suggests cloud variability due to effects of varying large-scale subsidence and midlatitude synoptic systems influencing the subtropical low cloud regime.

The region of pronounced variability east of 100°W between 5°S and the Equator is south of the sharp oceanic front and is largely a region of climatological warm-air surface layer temperature advection. Since the sign of meridional SST gradient and climatological temperature advection reverse at or just south of 0° the mean conditions in this area are different from those north of the front and, as a result, cloud variability differs as well.

Maps of correlation between some reanalysis atmospheric fields and low cloud amount serve as a starting point in diagnosing low cloud variability. In Fig. 2, the expected positive correlation between LTS and cloud amount anomalies is found for most of the climatological low-cloud region, although the relationship is statistically significant at the 95% level mainly in the southern region of the stratiform deck and on the northern edge of the domain, north of the equatorial SST front. A sizable area in the climatological low cloud region shows only weak positive correlation.

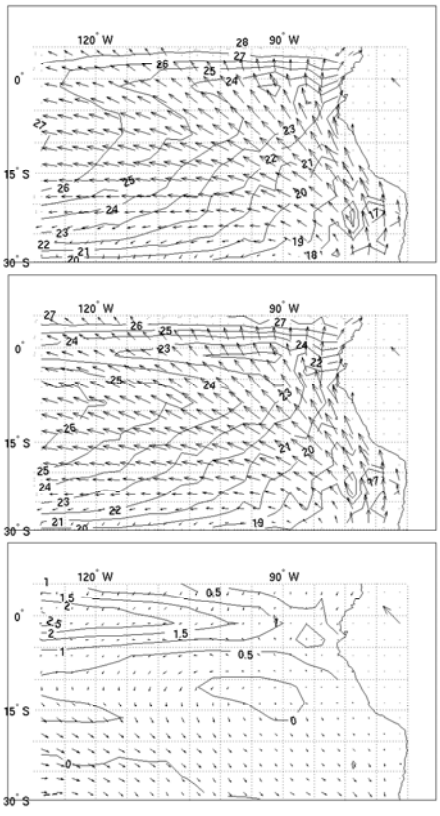

Fig. 5 Mean SST and winds for warm anomalous advection qunitile (top), cool anomalous advection quintile (middle), and cold-warm differences in anomalies (bottom). Vector in upper-right is 5 m s^{-1}.

As far as the low cloud-temperature advection relationship, there are regions of both positive and negative correlation. In general, we would expect a negative correlation between surface layer atmospheric temperature advection and low cloud amount anomalies, as cold advection helps form a more negative air-sea temperature difference, destabilizes the surface layer, increases latent and sensible heat fluxes, and allows for a continued supply of moisture above the lifting condensation level (LCL).

Surprisingly, in the middle panel, there is a large region in the climatological stratiform deck area where the correlation is positive, and while it is largely a weak correlation, some grid boxes show positive correlation at statistically significant levels. However, almost every grid box with such a positive cloud-advection correlation, and every one where the correlation is shaded, also shows a positive correlation between temperature advection and LTS.

So, the areas where anomalously warm advection correlates with increased low cloud amount are best thought of as areas where clouds respond to LTS changes more than to changes in temperature advection. Since interannual wind variability is small compared to SST variability in this region, anomalous temperature advection is dominated by mean winds advecting anomalous temperatures, while LTS is closely linked to SST. Thus, the distribution of SST anomalies, locally and over mean wind streamlines, largely dictates the sign of the both LTS and the temperature advection anomalies.

While the most negative temperature advection-cloud correlation is found north of the equator, there are also several areas south of the equator, over the cold tongue, where correlation is -0.3 or lower and is significant at the 95% level. Here, temperature advection and LTS are decidedly positively correlated, indicating that the expected effects on clouds imparted by LTS and those imparted by temperature advection are at odds with each other.

While correlation maps are telling about individual relationships, we turn to multilinear regression analysis to see how well the atmospheric temperature advection field, used in addition to LTS, accounts for low cloud amount variability. In Fig. 3 we see the amount of additional cloud variance that this second regressor accounts for. While in much of the domain it accounts for little extra variance, there is a distinct cold tongue box. spanning 105°-95°W, 5° S - 0° where temperature advection explains significantly more low-cloud variance than LTS alone. In this box the fraction of low cloud amount variance explained using both regressors is around 0.5. As noted, it is an area where LTS and temperature advection are positively correlated, meaning that the two fields tend to vary with each other in ways that imply opposing effects on low cloud.

Whether we use SST or LTS as the first regressor and, since variability of the wind field is small, whether we use temperature advection calculated from the actual reanalysis wind fields or calculated from actual SST and climatological mean wind fields as the second regressor, we find very similar patterns of increased R^2 statistic, with a distinct maximum in the 10°x5° and some

variation of the location of grid boxes significant at the 95% and 99% confidence levels. We do not find analogous patterns when repeating the calculations with regressor variables not directly related to LTS and temperature advection.

Fig. 4 shows ISCCP low cloud amount anomaly as a function of temperature advection and LTS anomalies in the 10°x5° cold tongue box. In the first panel, cloud amount anomaly increases downward along a column as well as to the right across any row, indicating a consistent tendency for increased cloudiness with cooler advection as well as with increased LTS. In contrast, data in the second panel from an area of the same size, spanning 95°-85°W, 30°-25°S, show a less consistent cloud response to anomalous atmospheric temperature advection. In this panel, cloud amount generally increases in any row with increasing LTS, but does not consistently increase with cooler temperature advection in any column.

In the cold tongue box, ENSO variability is associated with the SST gradient upwind and anomalous surface layer advection. As shown in Fig. 5, the mean SST and wind anomaly distributions for warm minus cold advection quintiles are similar to the patterns characteristic of classic El Niño events (e.g., Rasmusson and Carpenter 1982; Deser and Wallace 1990). As Table 1 shows, anomalous cold advection correlates with Niño 3.4 and with low cloud anomaly each at the 95% significance level. But low cloud and Niño 3.4 are only slightly correlated, and not by an amount significant at the 95% level. Since local SST within the box is significantly correlated with low cloud amount, it seems that an index of broad-scale SST anomalies such as Niño 3.4 does not project strongly on the ISCCP low cloud amount within this region. Note, though, that Park and Leovy (2004, Fig. 6) do show a statistically significant signal in this area for clear sky frequency and stratiform cloudiness in regressions of surface observations on their ENSO index.

The ISCCP and reanalysis data suggest that weakening of the equatorial cold tongue and anomalous cold advection help destabilize the surface layer and increase upward latent and sensible heat fluxes, transporting moisture above the LCL and increasing low-level cloudiness. Measurements of vertical fluxes in this region, taken in September 1996, appear in Paluch et al. (1999). About the SST front the vertical fluxes of latent and sensible heat vary greatly, with considerably greater values in warmer waters north of the front. There are similar results as well over an area of coastal upwelling near 10° S in the Paluch et al. study, where a stable surface layer is also clearly visible in certain soundings. We propose that on interannual scales as well, cold or weakened warm temperature advection discourages the formation of a stable surface layer and maintains upward latent heat fluxes, explaining the patterns found with the ISCCP data and regression analysis.

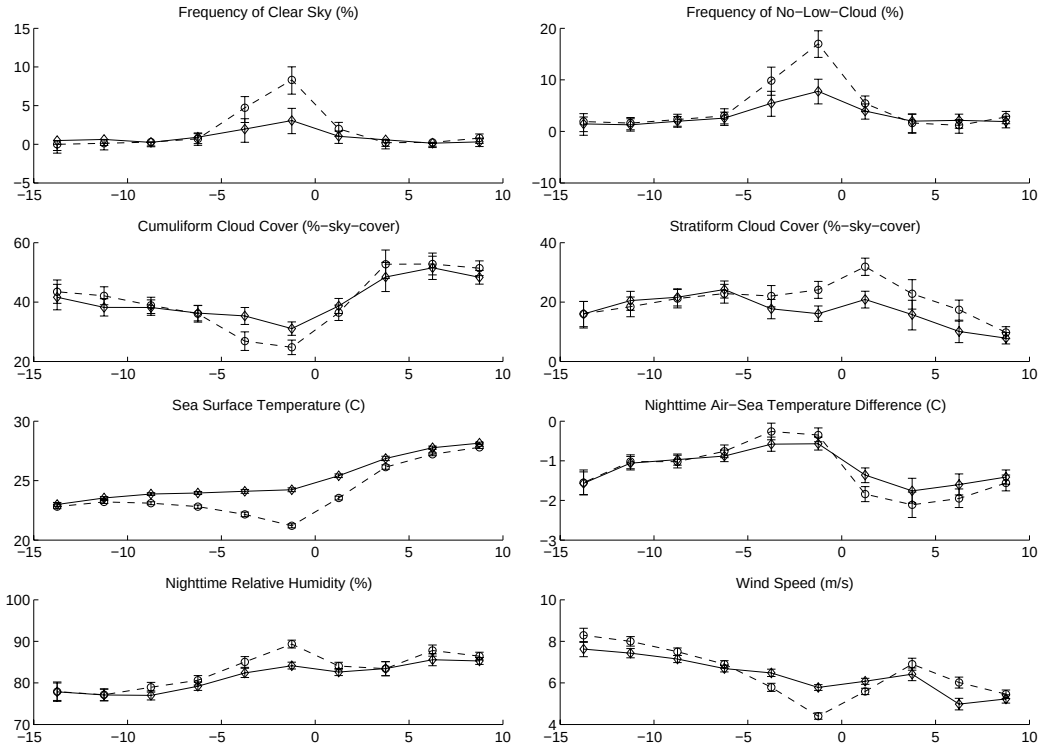

Fig. 6 Mean zonally averaged EECRA data for warm anomalous advection quintile months (dashed line) and cold quintile months (solid). Averaged over 105°-95°W.

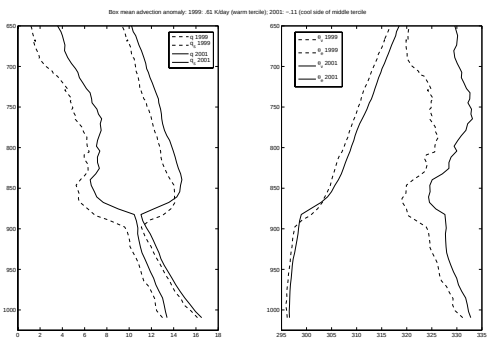

Fig. 7. Mean EPIC soundings for November 1999 and 2001, averaged as described in the text.

5. EECRA RESULTS AND SOUNDING DATA

The EECRA data add cloud type information to expand this hypothesis. Fig. 6 shows zonally averaged cross-sections of temperature advection quintile-mean data from EECRA. The data show markedly greater frequency of cloudless and no-low-cloud observations for the anomalously warm advection months than the cool quintile months. This part of the equatorial Pacific has a climatological local maximum of clear-sky observations (Park and Leovy 2004), and as Fig. 5 shows, the warm anomalous advection months correspond to a deepening of the climatological cold tongue and increased frequency of observed clear skies.

In the EECRA, cold-quintile months compared to warm averaged more cumuliform clouds (cumulus clouds of all sizes, including cumulus-under-stratocumulus, which indicate shallow convective activity in the MBL) over a latitude range including the cold tongue, by amounts significant at the 95% confidence level. Stratiform clouds (stratocumulus, stratus, and fog) are significantly more prevalent north of 6.25 S in the warm advection quintile months than in the cold.

ISCCP upper-level cloud	**-0.50**				
Niño 3.4	0.16	0.38			
Atm. temp. advection	**-0.46**	-0.25	**-0.77**		
Local SST	-0.28	**-0.76**	**0.74**	**-0.60**	
Lower-trop. Stability	0.36	**-0.73**	**-0.62**	**-0.62**	**-0.90**
	ISCCP low cloud	ISCCP upper-level cloud	Niño 3.4	Atm. Temp. advection	Local SST

Table 1. Correlation coefficients between reanalysis and ISCCP cloud fields. Correlations significant at the 95% level are in bold.

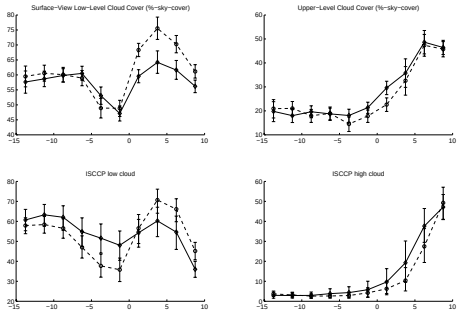

Fig. 8 As in fig. 6, but comparing EECRA (top) and ISCCP (bottom) data.

The EPIC sounding data during the months of November in 1999 and 2001 provide snapshots of the marine boundary layer during different advection scenarios. The mean surface layer advection during the two months was 1.22 K d^{-1} and 0.50 K d^{-1} with anomaly values of 0.61 K d^{-1} and -0.11 K d^{-1} corresponding to the warmest and the second coolest quintiles, respectively. In Fig. 7, mean data from soundings between 110°-95° W, 5° S - 0° show a distinct inversion in the temperature and moisture fields. Mean inversion heights were 1083 m and 1171 m and pressure levels were 898 and 876 hPa for 1999 and 2001, respectively. The warm-advection soundings show a low relative humidity just below the inversion, consistent with less vertical mixing, while the mean cold-advection sounding shows vapor pressure close to saturation. A deeper mean MBL and increase in 2001 compared to 1999 also correspond to a mean profile more common to cumulus or mixed Cu-under-Sc cloud environments, rather than just Sc, in subtropical soundings (Albrecht et al. 1995; Norris 1998a).

6. ZONAL AVERAGES FROM ISCCP

In Fig. 6, the cool advection anomaly months between 5° S and the Equator had significantly higher mean wind speed, more negative air-sea temperature difference, and lower relative humidity than the mean warm advection month EECRA observations. This supports the explanation that the warm advection months had a more stable surface layer, with less upward mixing of humidity and downward mixing of momentum, as postulated in Wallace et al. (1989). In Fig. 6, the cool advection anomaly months between 5° S and the Equator had significantly higher mean wind speed, more negative air-sea temperature difference, and lower relative humidity than the mean warm advection month EECRA observations. This supports the explanation that the warm advection months had a more stable surface layer, with less upward mixing of humidity and downward mixing of momentum, as postulated in Wallace et al. (1989).

In cool anomalous advection conditions in the 10x5° box, the surface layer is less stable and MBL is more well-mixed, allowing for shallow convection under the trade inversion as cumuliform clouds supplant stratiform. Since the stable surface layer leads to less mixing in warmer advection conditions, the greater amount of stratiform with no cumuliform clouds probably reflects remnant Sc clouds that formed in the more vertically well-mixed MBL south of the cold tongue and were advected into the area. As there are not always significant Sc clouds that persist as they are advected equatorward, formation of new clouds is strongly inhibited in warm advection conditions, and there is a pronounced tendency for clear and no-low-cloud observations over the cold tongue in these months.

In Fig. 8, both ISCCP and EECRA data show that cooler advection conditions (which have higher mean SST) contain more upper-level cloud north of 5° S. Since the cool advection scenarios tend to have warmer SST near the cold tongue, and given their positive correlation with ENSO indices and the mean contours in Fig. 5, this is consistent with a higher probability of deep convection and high clouds. In the ISCCP record, the zonally averaged low cloud amount is greater, by amounts significant at the 95% level, for anomalously cool advection months compared to warm between 5° S and the equatorial. North of the equatorial front the relationship is decidedly reversed, as the reversal of

Dataset and Longitude range		Mean temperature advection anomaly (K/day)		Mean low cloud anomaly (%)	
		Anomalously cool advection S of Eq	Anomalously warm advection S of Eq	Anomalously cool advection S of Eq	Anomalously warm advection S of Eq
ISCCP-reanalysis, 110°-90°W	Eq-5N	1.19	-0.47	-6.64	0.90
	5S-Eq	-0.87	0.71	3.38	-6.72
CCSM 130-110	Eq-5N	0.66	-0.76	13.50	-16.25
	5S-Eq	-1.72	1.82	13.11	-14.11
GFDL2.0 125-105°W	Eq-6N	0.20	-0.13	6.05	-5.52
	6S-Eq	-0.71	0.54	-1.93	1.53
GFDL 2.1 130-110°W	Eq-6N	0.30	-0.32	18.15	13.09
	6S-Eq	-1.30	1.03	4.01	-3.42
CCSM 110-90°W	Eq-5N	0.25	-0.03	3.81	-7.20
	5S-Eq	-0.27	0.25	4.43	-6.38
GFDL2.0 110-90°W	Eq-6N	0.06	0.16	2.30	-5.08
	6S-Eq	-0.28	0.23	0.61	-0.89
GFDL 2.1 110-90°W	Eq-6N	-0.17	0.49	8.86	-12.10
	6S-Eq	-0.40	0.39	4.02	-4.55

Table 2. Mean temperature advection anomaly and low cloud anomaly for the coldest and warmest temperature advection anomaly quintiles in regions about the cold tongue for observational and model data. In each case, the the quintile months are chosen based on advection anomaly values on the southern section of the region indicated.

SST gradient generally corresponds to anomalous advection of the other sign and cloud response described in Deser et al. (1993). In EECRA, anomalously warm versus cold advection is associated with opposing effects in stratiform and cumuliform clouds, and there is no clear, statistically significant tendency in zonally averaged total low cloud sky coverage over the range 105°-95° W.

The difference in total low cloud amount tendencies between ISCCP and EECRA are not a result of the random overlap correction; uncorrected ISCCP data yield very similar patterns (not shown) and confidence intervals up to 1.25° N. Moreover, the EECRA also calculates expected satellite-view sky cover by performing a random overlap correction on individual observations (Hahn and Warren 1999). These zonally averaged data (not shown) yield a pattern that is marginally different from that of the corrected data at 3.75° and 1.25° S, but which still is not statistically significant.

7. COMPARISON WITH MODEL DATA

The essential findings from the observational data sets are summarized in Table 2, which shows zonally averaged data composited based on the temperature advection anomaly quintiles south of the equator in the Eastern tropical Pacific from ISCCP and reanalysis data. In the observations, as shown in the table, the zonally averaged temperature advection and low cloud amount anomalies are of opposite sign within each area, and each quantity is of opposite sign on opposite sides of the Equator. In contrast, none of the three model data sets examined display both of these properties.

Over the first set of longitude ranges, the temperature advection anomaly did indeed vary out of phase across the equator in each model. In the CCSM model, there was no consistent response in low cloud anomaly; the advection-cloud relationship was negative south of the Equator, and positive to the North. Interestingly, the positive relationship was most strong north of the equator when advection there was cool.

With the CCSM model, maps (not shown) of the mean SST and surface winds for the warmest and coolest quintiles show that, as in the observations, the winds change comparatively little compared to the SST distributions. In this case, the winds maintain a southeasterly orientation even well north of the Equator over the range 110° -130° W near the equator. The change in temperature advection corresponds to a strong cold equatorial SST area centered just east of 110°W. The easterly component of the winds advects the anomalously cool air over the compositing area, while the southerly component over the model's equatorial cold tongue explains the out-of-phase variation of temperature advection across the Equator.

The fact that the CCSM model shows consistent cloud anomalies across the equator in this region suggests that the low clouds might correspond to the bases of deeper convecting clouds, in months when convergence zones are near the equator. However, examinations of CCSM mean low and upper-level cloud maps (not shown) demonstrate no such correlation between low and upper-level cloud or cloud anomaly behaviors; the low clouds registered in CCSM data can be thought of as stratiform or shallow cumulus clouds, not the bottoms of towering cumulus. Equivalent maps for the GFDL 2.0 and GFDL 2.1 models (not shown) show similar mean SST distributional changes with small variations in surface winds between the warm and cool advection scenarios. Essentially, the models show anomalously warm and cold surface-layer temperature advection corresponding to cold tongue strengthening and weakening just as in observations, with a westward shift in the area of high variability corresponding to a detached cold tongue. While the mechanism of cross-equatorial surface winds and equatorial SST variability leads to realistic temperature advection variability, the unrealistic model low-level cloud response suggests the need to improve cloud physics and boundary layer schemes.

8. CONCLUSIONS

ISCCP data show that the eastern Pacific south of the Equator exhibits pronounced low cloud variability on interannual time scales. SST and LTS explain some of the variance in low cloud amount, but atmospheric temperature advection also plays an important role in cloud type, frequency, and cloud amount over the cold tongue, especially over the region extending approximately 1500 kilometers west from the Galápagos.

Both EECRA and ISCCP data indicate that when surface layer atmospheric temperature advection is warm, the stable surface layer and diminished fluxes from the sea surface inhibit vertical mixing in the MBL. This is evident not only in the ensuing cloud changes but also in the comparatively stagnant surface layer, which has greater humidity and less winds than in cold advection conditions, and in the less negative air-sea temperature differences. The EECRA data indicate that warm advection conditions are conducive to skies with remnant stratocumulus clouds or cloudless conditions, as less moisture is being brought above the LCL, and the EPIC soundings confirm that during cool temperature advection conditions an MBL structure more characteristic of cumuliform clouds prevails.

However, the EECRA and ISCCP cloud data sets are at odds regarding the effect of interannual temperature advection variations on total low cloud amount anomalies. While cooler advection corresponds to greater low cloud coverage in ISCCP, in EECRA there is no clear trend.

The cloud response to atmospheric temperature advection found in observations is not reproduced in models. Since vertical resolution is still far away from resolving the skin layer versus the surface layer (i.e., the bottom several meters of the atmosphere) and the ensuing air-sea temperature differences and thermally driven turbulent fluxes, models could use parameterizations based on temperature advection, as well as information of actual SST and other factors, to improve low cloud simulation.

The ways described here in which low clouds show discernible response to anomalies in fields other than LTS also pertain to regional ocean-atmosphere

processes over coastal upwelling areas, as well as to past or future climates whose cold tongue mean characteristics or variability differ from todays. The apparent inconsistencies between ISCCP and EECRA data, as well as the trends identified in cloud type and boundary layer data in EECRA and EPIC soundings, could hold more general relevance to studies of boundary layer transition equatorward of the subtropics. Additionally, the variability described here can serve to constrain models that aim to capture boundary-layer dynamics, cloud-topped MBL behavior, and cloud feedbacks in global climate.

Acknowledgements. This work was supported by NSF CAREER grant AM02-38257, NASA grant GWEC NAG5-11731, and DOE grants DE-FG03-01ER63255 and DE-FG02-04ER63857. The first author was also assisted by a California Space Institute/Space Grant fellowship. The authors are grateful to Nick Bond of NOAA/PMEL for EPIC soundings.

REFERENCES

Bolton, D., 1980: The computation of equivalent potential temperature. *Monthly Weather Rev.*, **108**, 1046-1053.

Collins, W. D., C. M. Bitz, M. L. Blackmon, G. B. Bonan, C. S. Bretherton, J. A. Carton, P. Chang, S. C. Doney, J. J. Hack, T. B. Henderson, J. T. Kiehl, W. G. Large, D. S. McKenna, B. D. Santer, and R. D. Smith, 2005: The community climate system model: CCSM3, submitted, *J. Climate*.

Delworth, T. L., A. J. Broccoli, A. Rosati, R. Stouffer, V. Balaji, J. A. Beesley, W. F. Cooke, K. W. Dixon, J. Dunne, K. D. J. W. Durachta, K. L. Findell, P. Ginoux, A. Gnanadesikan, C. T. Gordon, S. M. Griffies, R. Gudgel, M. J. Harrison, I. M. H. andR. S. Hemler, L. W. Horowitz, S. A. Klein, T. R. Knutson, P. J. Kushner, A. R. Langenhorst, H. C. L. amd S. J. Lin, J. Lu, S. L. Malyshev, P. C. D. Milly, V. Ramaswamy, J. Russell, M. D. Schwarzkopf, E. S. dn J. J. Sirutis, M. J. Spelman,W. F. Stern, M.Winton, A. T.Wittenberg, B. Wyman, and F. Z. and R. Zhang, 2005: GFDL's CM2 global coupled climate models . Part 1: Formulation and simulation characteristics. Revised, *J. Climate*.

Deser, C., J. J. Bates, and S. Wahl, 1993: The influence of sea-surface temperature-gradients on stratiform cloudiness along the equatorial front in the Pacific Ocean. *J. Climate*, **6**, 1172-1180.

Deser, C. and J. M. Wallace, 1990: Large-scale atmospheric circulation features of warm and cold episodes in the tropical Pacific. *J. Climate*, **3**, 1254-1281.

Hahn, C. J. and S. G. Warren, 1999: Extended edited synoptic cloud reports from ships and land stations over the globe, 1952-1996. Numerical Data Package NDP026C, Carbon Dioxide Information Analysis Center, Oak Ridge National Laboratory, Oak Ridge, TN 37831-6335, 71 pp.

Kalnay, E., M. Kanamitsu, R. Kistler, W. Collins, D. Deaven, L. Gandin, M. Iredell, S. Saha, G. White, J. Woollen, Y. Zhu, M. Chelliah, W. Ebisuzaki, W. Higgins, J. Janowiak, K. C. Mo, C. Ropelewski, J. Wang, A. Leetmaa, R. Reynolds, R. Jenne, and D. Joseph, 1996: The NCEP/NCAR 40-year reanalysis project. *Bull. Amer. Meteor. Soc.*, **77**, 437-471.

Klein, S. A., D. L. Hartmann, and J. R. Norris, 1995: On the relationships among low-cloud structure, sea-surface temperature, and atmospheric circulation in the summertime northeast Pacific. *J. Climate*, **8**, 1140-1155.

Norris, J. R., 1998a: Low cloud type over the ocean from surface observations. Part I: relationship to surface meteorology and the vertical distribution of temperature and moisture. *J. Climate*, **11**, 369-382.

Norris, J. R., 1998b: Low cloud type over the ocean from surface observations. Part II: geographical and seasonal variations. *J. Climate*, **11**, 383-403.

Pyatt, H. E., B. A. Albrecht, C. Fairall, J. E. Hare, N. Bond, P. Minnis, and J. K. Ayers, 2005: Evolution f marine atmospheric boundary layer structure across the cold tongue-ITCZ complex. *J. Climate*, **18**, 737-753.

Ramanathan, V., R. D. Cess, E. F. Harrison, P. Minnis, B. R. Barkstrom, E. Ahmad, and D. Hartmann, 1989: Cloud-Radiative Forcing and Climate: Results from the Earth Radiation Budget Experiment. *Science*, **243**, 57-63.

Rossow,W. B. and R. A. Schiffer, 1999: Advances in Understanding Clouds from ISCCP. *Bulletin of the American Meteorological Society,* **80**, 2261-2288.

Rozendaal, M. A., C. B. Leovy, and S. A. Klein, 1995: An observational study of diurnal variations of marine stratiform cloud. *J. Climate*, **8**, 1795-1809.